Fast and Broadband Photonic Integrated Microwave Phase Shifter

G. Serafino[1], C. Porzi[1], M. Sans[3], F. Falconi[2], V. Sorianello[2], S. Pinna[1], M. Romagnoli[2], John E. Mitchell[3], A. Bogoni[1,2], P. Ghelfi[2]

[1]*TeCIP – Scuola Superiore Sant'Anna, Pisa, Italy*
[2]*CNIT – National Photonics Labs, Pisa, Italy*
[3]*Department of Electronic and Electrical Engineering – University College London, London, UK*
e-mail: c.porzi@sssup.it, paolo.ghelfi@cnit.it

Abstract: An integrated silicon-on-insulator microwave photonic phase shifter based on an optical deinterleaver and a reverse-biased pn-junction waveguide providing broadband phase shifts over more than 360° with an ultrafast reconfiguration time of 1 ns is demonstrated.
OCIS codes: (130.3120) Integrated optics devices; (060.5625) Radio frequency photonics;

1. Introduction

Microwave-photonic phase shifters (MWP-PSs) enable processing of radio-frequency (RF) signals in radio-over-fiber communications, sensing, and defense systems, with the advantages of broadband operation, large phase-shift ranges, and immunity to electromagnetic interference in respect to their electronic counterparts. Additionally, a fast response time is an appealing feature for forthcoming 5G systems, where fast MWP-PSs can be exploited to implement rapidly reconfiguring beam-steering in phased-array antennas. For practical system applications, on-chip integration is also desirable due to increased stability, extremely minimized encumbrance and weight, and low operating power of photonic-integrated circuits (PICs). To this aim, several PICs implementing MWP-PSs have been proposed in the last recent years [1]-[4], none of them simultaneously matching the demand for wide phase-shift range, broad bandwidth, low in-band power oscillations, ultra-fast (i.e., sub-μs) reconfiguration time, and compatibility with CMOS integrated circuits fabrication technology.

Here, we present a photonic-integrated MWP-PS realized in CMOS-compatible silicon-on-insulator (SOI) technology, performing stable phase shifts well in excess of 360° over a bandwidth of 6 GHz for RF carriers spanning in the x- and k-band, with in-band power variations within 1 dB and fast response time of less than 1 ns.

2. Integrated MWP-PS Operation Principle Implementation, and Results

The schematic operation of the MWP-PS is shown in Fig. 1(a); the circuit comprises an optical deinterleaver filter (ODF), an optical phase shifter (OPS) element, an optical coupler (OC), and balanced photodiodes (BPDs). The ODF spatially separates an optical carrier from a signal sideband generated by modulating the optical frequency ν_c emitted by a laser source (LS) through a single-sideband electro-optic modulator (SSB-EOM) driven by the microwave signal centered at f_{RF}. After the ODF, the isolated optical carrier traverses the OPS, before being recombined with the un-shifted modulated sideband and being photo-detected. The signal–sideband beating at the BPDs then translates the phase-shift applied to the optical carrier by the OPS to the down-converted RF signal.

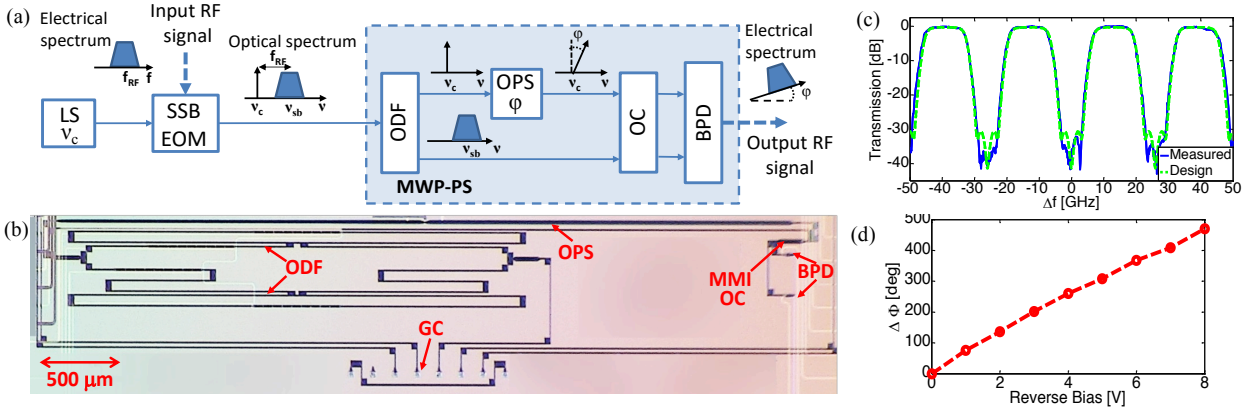

Fig. 1. (a): Photonic-based microwave-photonic (MWP) PS operation; LS: laser source; SSB-EOM: single-sideband electro-optic modulator; ODF: optical deinterleaver filter; OPS: optical phase-shifter; OC: optical coupler; BPD: balanced photodiodes. (b): Optical image of the fabricated PIC realizing the photonic microwave PS. (c): Measured transmission spectrum and target design simulation of the ODF; (d): Measured integrated OPS characteristic.

A PIC, realizing the scheme within the dashed box of Fig. 1(a), has been fabricated in SOI technology through a multi-project wafer run [5]. An optical image of the fabricated PIC is shown in Fig. 1(b). A microring resonator-loaded Mach-Zehnder interferometer realizes the ODF. The OPS exploits carrier depletion-induced effective index modulation in a 4.25 mm-long interdigitated pn junction embedded in a rib waveguide. A multimode-interference (MMI) OC is used to couple the modulated sideband and the phase-shifted optical carrier before *p-i-n* germanium BPDs with -3dB bandwidth of ~18 GHz. Grating couplers (GCs) are used for vertical coupling with the accessing input optical fiber. The transmission of the ODF at one output port is reported in Fig. 1(c), showing a periodic box-like transmission with steep roll-off and a free-spectral-range (FSR) of 26 GHz exhibiting a flat passband with a -0.5 dB bandwidth of ~8 GHz and a -30 dB stop-band width of ~6.5 GHz. The characteristic of the OPS is reported in Fig. 1(d), where a 475° phase shift over a range of 8V for the pn-junction reverse bias is measured.

The integrated MWP-ps has been characterized using the set-up of Fig. 2(a); the output frequency from a vector network analyzer (VNA) has been swept over a bandwidth of 6 GHz centered at f_{RF}=13 GHz, to generate the SSB signal entering the PIC. An erbium-doped fiber amplifier (EDFA) boosts the signal power at PIC input up to ~10 dBm. A polarization controller (PC) optimizes the chip coupled power through the GC. The LS optical carrier is initially tuned in the center of the ODF passband transmission toward the OPS branch. The microwave signal at the PIC output is delivered back to the VNA. The magnitude and phase of the measured S_{21} parameter are shown in Fig. 2(b), where electrical phase-shifts constant between 10 and 16 GHz ranging over more than 450° when the bias voltage is swept between 0V and 8V are observed. The standard deviation of the measured phase response over the full bandwidth range stays below 1.5° for a full 360° span. Due to the squared ODF transmission, the power oscillations over the whole 6 GHz bandwidth are confined well within 1 dB. By tuning the optical carrier from the LS at the edges of the ODF passband, similar characteristics over a 6 GHz sweep span around f_{RF}=10 GHz and f_{RF}=16 GHz have been observed.

The interdigitated pn-junction implementing the OPS has an intrinsic unit-length bandwidth of several tens of GHz, which is however limited by the lumped-electrode load resistance in this relatively long structure. The modulation bandwidth of the OPS has then been characterized by connecting the LS output to the PIC, and tuning the ODF such that the light is almost evenly split between the two branches of the circuit, producing phase-to-intensity modulation conversion when it recombines in the OC. By using a bias-tee to properly bias the OPS and prevent forward-biasing of the pn-junction, and applying to the OPS a square-wave signal with amplitude of 2V (corresponding to ~0.7π phase shift) generated by a waveform generator, the step response of the MWP-PS has been, measured by monitoring the photodetected output waveform on a sampling oscilloscope. The results are illustrated in Fig. 3(b), where details of the rising and falling edges are also illustrated, for a measured rising time, τ_r, below 1 ns

3. Acknowledgements

This work has been carried out within the EU project FiWin5G (#642355) and the Italian national projects PREVENTION (with the contribution of the Ministry of Foreign Affairs) and PHOOD.

4. References

[1] M. Pagani, et al "Tunable wideband microwave photonic phase shifter using on-chip stimulated Brillouin scattering," Opt. Express **22,** 28811-28818 (2015).

[2]Tang, Jian, et al. "Broadband microwave photonic phase shifter based on a feedback-coupled microring resonator with small radio frequency power variations." Optics letters 41.20 (2016): 4609-4612.

[3] M. Burla, et al. "On-chip programmable ultra-wideband microwave photonic phase shifter and true time delay unit," Opt. Lett. **39**, 6181-6184, (2014).

[4] V. J. Urick et al., "Microwave Phase Shifting Using Coherent Photonic Integrated Circuits," IEEE J. Sel. Topics Quantum Electron. **22**, 353-360 (2016).

[5] "Europractice Multi Project Wafer," http://www.europractice-ic.com/ SiPhotonics_technology_imec_ISIPP25G.php.